Applied Physics Express **5** (2012) 012102
DOI: 10.1143/APEX.5.012102

Genetic Algorithm for Innovative Device Designs in High-Efficiency III–V Nitride Light-Emitting Diodes

Di Zhu, Martin F. Schubert, Jaehee Cho*, E. Fred Schubert, Mary H. Crawford[1], Daniel D. Koleske[1], Hyunwook Shim[2], and Cheolsoo Sone[2]

Department of Electrical, Computer, and Systems Engineering, Rensselaer Polytechnic Institute, Troy, NY 12180, U.S.A.
[1]*Sandia National Laboratories, Albuquerque, NM 87185, U.S.A.*
[2]*R&D Institute, Samsung LED, Suwon, Gyeonggi 443-744, Korea*

Received September 22, 2011; accepted December 8, 2011; published online January 5, 2012

Light-emitting diodes are becoming the next-generation light source because of their prominent benefits in energy efficiency, versatility, and benign environmental impact. However, because of the unique polarization effects in III–V nitrides and the high complexity of light-emitting diodes, further breakthroughs towards truly optimized devices are required. Here we introduce the concept of artificial evolution into the device optimization process. Reproduction and selection are accomplished by means of an advanced genetic algorithm and device simulator, respectively. We demonstrate that this approach can lead to new device structures that go beyond conventional approaches. The innovative designs originating from the genetic algorithm and the demonstration of the predicted results by implementing structures suggested by the algorithm establish a new avenue for complex semiconductor device design and optimization.

Light-emitting diodes (LEDs) are the driving force behind solid-state lighting with its explosive growth in illumination applications. Efforts in identifying high-performance LED structures have focused on optimizing single aspects of the devices. However, a multivariable LED system exhibits an enormous parameter space with strong cross-coupling between the structural parameters of an LED. Therefore, LED device optimization by conventional iterative design processes can be inefficient in identifying a truly optimized structure.

Here, we address the search for efficient LED structures by introducing an artificial evolutionary strategy, an approach that complements a III–V nitride device simulation package with a genetic algorithm (GA) tailored for semiconductor device optimization. We demonstrate that the GA can efficiently search for innovative yet realizable LED structures by focusing on the (i) multiple-quantum-well (MQW) active region and (ii) electron-blocking layer (EBL) of an LED. The result, i.e., an LED with an optimized MQW, is tested quantitatively by a series of experimental studies. Furthermore, an advanced EBL structure has emerged from the GA, with the promise of significantly reducing electron leakage and enhancing device efficiency.

A GA, a heuristic search method inspired by the concept of evolution, employs natural *selection* and *reproduction*.[1,2] Selection is accomplished by using LED simulation software that, based on a specific performance criterion, assigns a fitness value to a particular device structure; this value forms the basis of the GA's natural selection process. Reproduction is accomplished by cloning, crossover, and mutation to generate novel and unanticipated solutions for the LED optimization problem. This capability makes the GA particularly suitable for optimizing complex and coupled multivariable systems such as LEDs. Although the GA has been applied to bioinformatics,[3] atomic clusters,[4] material interfacial structures,[5] neural networks,[6] and optical antireflection coatings,[7] we show that the employment of a GA can yield insightful and revolutionary guidance for advanced semiconductor device designs.

A typical LED structure includes the substrate, n-type GaN, MQWs, spacer, EBL, and p-type GaN layers, as shown in Fig. 1(a). In the implementation process of the GA, an initial group (population) of LEDs (individuals) is created with the material composition, thickness, and doping concentration of each layer randomly generated or based on conventional designs. The entire population is first evaluated by the device modeling software SDSIM (Semiconductor Diode Simulator Implemented in Matlab). SDSIM is an in-house simulation package that self-consistently solves the Poisson and carrier-transport equations under equilibrium and non-equilibrium conditions. SDSIM allows the calculation of the electronic structure of individual III–nitride materials as well as the modeling of the band diagram, carrier concentration and recombination, and current–voltage characteristic in a device structure. Some material and device parameters which are used in our calculations are listed in ref. 8.

After the evaluation, the entire population is then graded (i.e., rank-ordered) according to a fitness function. In our case, the fitness function is the internal quantum efficiency

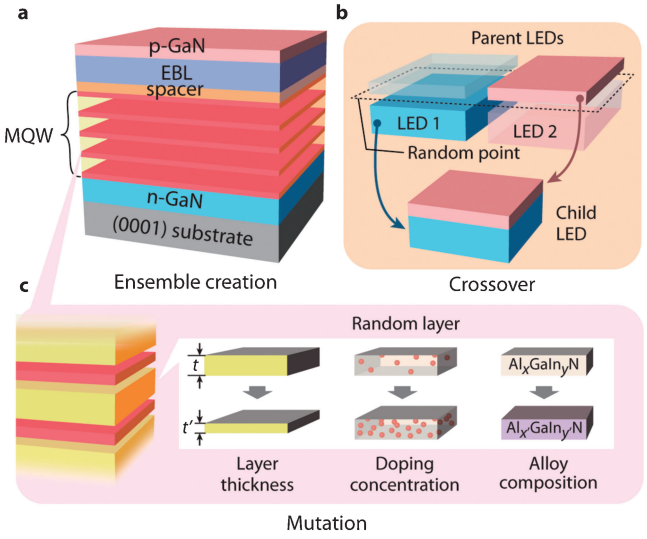

Fig. 1. (a) Typical LED structure used in the GA with n-type GaN, MQWs, spacer, EBL, and p-type GaN layers on (0001) sapphire. (b) Illustration of the crossover strategy for generating new child LEDs. (c) Illustration of the mutation process showing three different ways of changing the parameters of a random layer.

*E-mail address: choj6@rpi.edu

(IQE) multiplied by a weight function giving more emphasis to IQE values at high current density, i.e.,

$$\text{Fitness function} = \text{IQE}_{\text{High}}\left(\frac{\text{IQE}_{\text{High}}}{\text{IQE}_{\text{Peak}}}\right)^2,$$

where IQE_{Peak} is the peak IQE, and IQE_{High} is the IQE at a high current density. From the definition of this fitness function, it is demanded for the optimal LED structure to have an as high as possible efficiency (the first factor of the product) and also the second factor of the product (i.e., a small efficiency droop). Following that, the fittest individuals of the population are selected and copied (cloned) or modified by the variation-inducing operations of crossover and mutation, as illustrated in Figs. 1(b) and 1(c), respectively. The process is repeated until a termination condition is met. Crossover is the method of combining selected individuals into new individuals. In the crossover stage [Fig. 1(b)], devices from the current generation are randomly paired as "parents". A crossover point is then chosen at a random layer interface that splits up the two "parent" LEDs. The "child" LED is then created by exchanging and recombining the layers above the random point of one parent LED and the layers below the random point of the other parent LED. In the mutation [Fig. 1(c)], one layer is randomly selected and modified. The modifications include either increasing or reducing the layer thickness, doping concentration, and alloy composition, and we refer to all these modifications as mutations. In addition to crossover and mutation, a cloning strategy is applied that simply preserves the best individuals from the current generation, and these individuals are directly passed on to the next generation without changes. The GA is normally executed for up to 500 generations with a typical population size of 1000.

The MQW is the central region of LEDs where emission occurs after carriers are captured, confined, and recombined in the quantum wells (QWs). It was reported that carrier transport in the MQWs can be greatly affected by the quantum barriers (QBs).[9,10] Here, we focus on optimizing the QB doping in a five-period MQW LED, and we allow the GA to vary the doping in each of the QB layers from undoped to n-type doped up to $1 \times 10^{19}\,\text{cm}^{-3}$. A fixed GaN QB thickness of 8 nm and a regular 30-nm-thick p-type AlGaN EBL are used. The optimized LEDs suggested by the GA show low QB doping comparable to the background doping concentration of undoped GaN ($\sim 10^{16}\,\text{cm}^{-3}$). To validate this theoretical result, we have grown four LEDs with a different number of undoped QBs in the active region. The five-period MQW region consists of 2.5-nm-thick QWs and 8.2-nm-thick QBs. The light–output power (LOP) of the four LEDs is measured at current densities of 200, 300, and 500 A/cm^2, as shown in Fig. 2(a). The results show that the all-QB-doped LED shows the lowest LOP; LOP gradually increases as more QBs are undoped. At the current density of 500 A/cm^2, the measured LOP of the one-QB-doped LED is 31% higher than the all-QB-doped LED. These measurements are in excellent agreement with the prediction of the GA. Note that although it has long been believed that the QBs of a GaInN/GaN MQW LED structure should be doped to attain high efficiency,[11,12] we show experimentally, as well as theoretically, that undoped QBs are better in terms of reducing the efficiency droop.

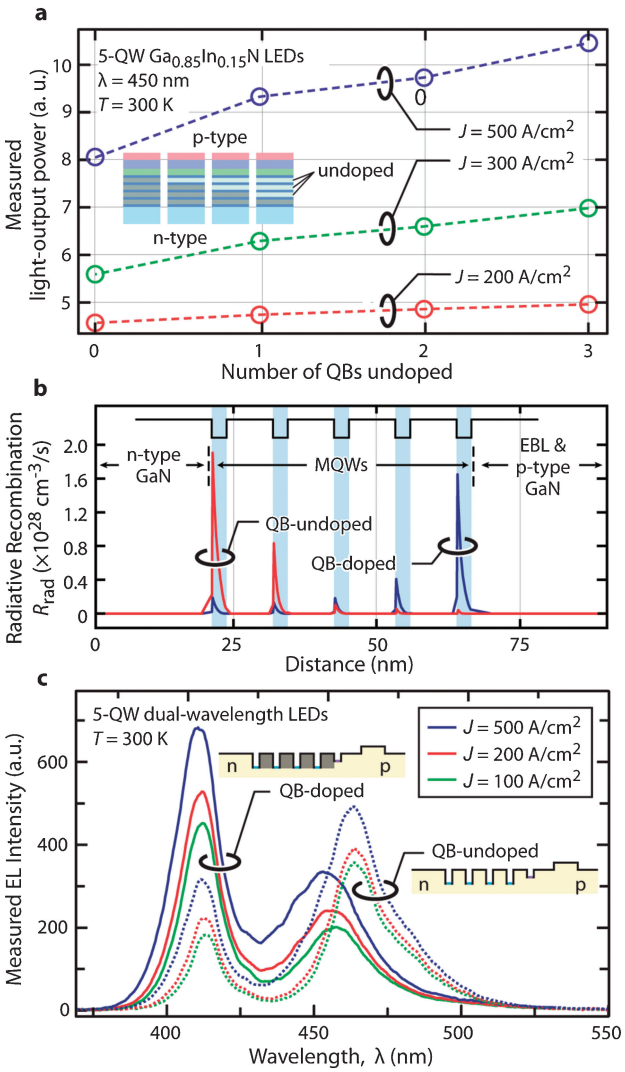

Fig. 2. (a) Measured light–output power of the LEDs with different numbers of undoped QBs at current densities of 200, 300, and 500 A/cm^2. (b) Simulated distribution of radiative recombination among the MQWs of QB-undoped and -doped LEDs. (c) Measured spectra of QB-undoped and -doped dual-wavelength LEDs at current densities of 100, 200, and 500 A/cm^2.

The GA suggests that the high-current LOP can be enhanced by doping fewer QBs, so that the center of radiative recombination shifts away from the QW that is closest to the p-side towards the n-side, resulting in much less electron leakage out of the MQWs. The calculated distribution of radiative recombination in the MQWs of QB-doped and QB-undoped LEDs is shown in Fig. 2(b). To confirm the beneficial carrier distribution of the undoped barrier design, we experimentally investigate the distribution of radiative recombination by using dual-wavelength LEDs with an active region emitting at two distinguishable wavelengths. The two LEDs (one having doped QBs and the other undoped QBs) used in our study consist of four blue QWs and one violet QW located at the p-side. The measured spectra of the LEDs show strong violet peaks in the QB-doped LED, indicating that the majority of radiative recombination takes place in the p-side QW, whereas a stronger blue emission is observed in the QB-undoped LED. Notably, LEDs reported in the literature are demonstrated to

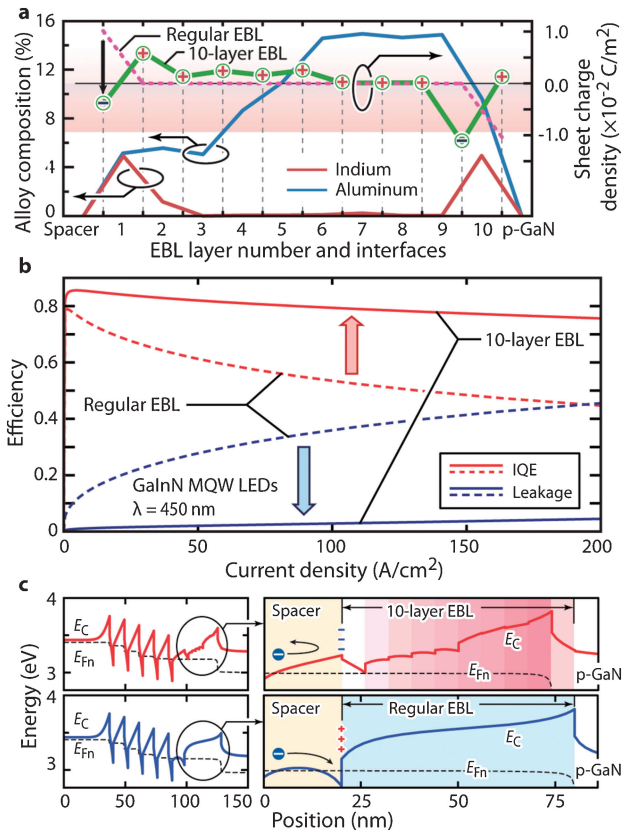

Fig. 3. (a) Plot of the Al and In composition given by the GA, together with the calculated interface sheet charge density of the 10-layer and regular EBL structures. (b) Calculated EQE and electron leakage efficiency versus the forward current density of the 10-layer and regular EBL structures. (c) Simulated conduction band diagrams including the MQW, spacer and EBL regions of the 10-layer and the regular EBL structures at a current density of 200 A/cm^2.

most commonly have only the dominant p-side QW emission under electrical pumping.[13] This condition is very different from the optimal carrier distribution proposed by the GA. The dual-wavelength LEDs therefore provide powerful evidence that the GA approach yields highly useful predictions in identifying device designs for improved performance over existing designs.

The EBL is another critical region that prevents electron leakage out of the active region to the p-type GaN region. Here, we report the device design of the EBL based on the GA. To simplify the design of the EBL, we limit the GA to a ten-layer p-type AlGaInN EBL with a fixed 3 nm thickness of each layer. The Al and In compositions are allowed to vary from 0 to 15% and from 0 to 5% in each layer, respectively. As a result, a novel EBL structure with a complex alloy composition scheme is suggested by the GA. Figure 3(a) shows plots of the Al and In alloy compositions of each layer in the optimized EBL. The corresponding interface sheet charge density (solid black line), as well as that of conventional single AlGaN EBL (dashed line), at each interface is also shown in Fig. 3(a). The GA introduces significant In content at the two sides of the EBL, possibly to reduce the polarization mismatch between the EBL and the nearby GaN spacer and p-type cladding layer. Note that the proposed EBL structure is not polarization-matched to the GaN. Instead, the interface sheet charge at the spacer-EBL interface is *inverted*, i.e., negative, compared with that of a regular AlGaN EBL, where the sheet charge is positive. This inverted interface sheet charge has never before occurred in conventional EBLs. In addition, the optimized structure shows Al composition grading at the center of the EBL.

The new EBL structure causes a 76% reduction in the calculated efficiency droop at 200 A/cm^2 compared with the conventional single-layer AlGaN EBL; the reduction in droop is primarily attributed to the reduced electron leakage, as shown in Fig. 3(b). To better understand this novel EBL structure, the conduction band diagrams are calculated at a current density of 200 A/cm^2 and compared with that of the regular EBL, as shown in Fig. 3(c). The reduction of electron leakage by the optimized EBL can be explained by the electron-repelling property of the negatively charged spacer-EBL interface. The opposite direction of electric field in the spacer layer can avoid extracting electrons from the MQWs and more effectively reduce the electron leakage into the p-type GaN compared with the positively charged regular spacer-EBL interface, which prevails in most EBL structures regardless of the Mg doping, Al composition, or EBL thickness used. With respect to the proposed new EBL structure, experimental verification is under way and will be separately reported in a future article.

In conclusion, the combination of GA handling the evolution and reproduction of a semiconductor device structure with device-simulation software handling the fitness and selection is shown to be applicable to designing and optimizing semiconductor devices. Our results are the starting point of applying artificial evolution to practical semiconductor devices, open new perspectives for complex semiconductor device optimization, and enable breakthroughs in high-performance LED design.

Acknowledgments The contributions including epitaxial growth of LED wafers by Sandia's Solid-State Lighting Science Center, an Energy Frontier Research Center funded by the U.S. Department of Energy, Office of Science, Office of Basic Energy Sciences, are greatly appreciated. The RPI authors gratefully acknowledge the support from Sandia National Laboratories, Samsung LED, and National Science Foundation. Sandia is a multi-program laboratory managed and operated by Sandia Corporation, a Lockheed Martin Company, for the US DOE's National Nuclear Security Administration under Contract No. DE-AC04-94AL85000.

1) J. H. Holland: *Adaptation in Natural and Artificial Systems* (MIT Press, Cambridge, MA, 1992).
2) D. E. Goldberg and K. Deb: in *Foundations of Genetic Algorithms I*, ed. G. J. E. Rawlins (Morgan Kaufmann, San Mateo, CA, 1991).
3) F. H. van Batenburg *et al.*: J. Theor. Biol. **174** (1995) 269.
4) D. M. Deaven and K. M. Ho: Phys. Rev. Lett. **75** (1995) 288.
5) A. L.-S. Chua *et al.*: Nat. Mater. **9** (2010) 418.
6) D. F. Cook *et al.*: Eng. Appl. Artif. Intell. **13** (2000) 391.
7) D. J. Poxson *et al.*: Opt. Lett. **34** (2009) 728.
8) Auger coefficient $\sim 10^{-31}$ cm^6/s; The radiative lifetime τ_R is determined by radiative coefficient B, carrier concentration n, and active volume V by following the formula $\tau_R = 1/(Bn^2V)$. Radiative coefficient B is 2.14×10^{-11} cm^3/s for $Ga_{0.85}In_{0.15}N$ QW; Non-radiative lifetime τ_{NR} for electron and hole in the quantum well are 44.6 and 264 ns, respectively.
9) D. Zhu *et al.*: Appl. Phys. Lett. **94** (2009) 081113.
10) J. Xie *et al.*: Appl. Phys. Lett. **93** (2008) 121107.
11) Y. Narukawa *et al.*: Jpn. J. Appl. Phys. **41** (2002) L371.
12) M. Yamada *et al.*: Jpn. J. Appl. Phys. **41** (2002) L1431.
13) A. David *et al.*: Appl. Phys. Lett. **92** (2008) 053502.